Assembly of Mesoporous Silica Molecular Sieves Based on Nonionic Ethoxylated Sorbitan Esters as Structure Directors

Eric Prouzet,*,† Frederic Cot,† Georges Nabias,† André Larbot,†
Patricia Kooyman,‡ and Thomas J. Pinnavaia§

Laboratoire des Matériaux et Procédés Membranaires (CNRS UMR 5635), ENSCM, 8 rue de l'Ecole Normale, F-34296 Montpellier Cedex 5, France, National Centre for HREM, Delft University of Technology, Rotterdamsweg 137, 2628 AL Delft, The Netherlands, and Department of Chemistry and Center for Fundamental Materials Research, Michigan State University, East Lansing, Michigan 48824

Received October 23, 1998. Revised Manuscript Received February 23, 1999

A new family of mesoporous silica molecular sieves with micelle-templated structures (MTS) has been synthesized using nonionic ethoxylated sorbitan esters, namely, Tween-20, -40, -60, or -80, as structure-directing agents. These MTS materials possess a wormhole-like framework typical of MSU-*X* mesostructures, with intraparticle (framework) pore sizes in the 3.0−4.0 nm range. Unlike previously reported MSU-*X* silicas, these new derivatives form monodispersed small particles in the 30−60 nm range, depending on the nature of the surfactant, and exhibit substantial interparticle (textural) porosity in the 9−20 nm range. The sorbitan surfactants are nontoxic, biodegradable, and biocompatible when solvent free, making them attractive structure directors for the synthesis of mesoporous materials. The combination of complementary framework and textural pore distributions should be advantageous in the use of the mesostructures as heterogeneous catalysts, particularly for reactions that are normally diffusion limited.

I. Introduction

Following the discovery of ordered mesoporous M41S materials,[1−3] considerable effort has been invested in expanding this new family of micelle-templated structures (MTS) by testing different synthesis pathways based on different structure-directing agents or reaction mechanisms. These structures rely on surfactant micelles or liquid crystals as structure-assembling agents (templates), which interact with inorganic precursors that will segregate and polymerize.[4,5] Assembly can involve charge density matching mechanisms between the surfactant and the silicate, mostly involving long-chain ammonium salts,[1,2,4−6] complexation,[7,8] preformed surfactant assembly,[9,10] or hydrogen bonding between electrically neutral inorganic entities and molecules such as amines[11,12] or nonionic poly(ethylene oxide) (PEO) based surfactants or block copolymers.[13−18] MTS materials assembled from PEO surfactants have been named MSU-*X* (*X* denotes the surfactant type) silica materials. Compared with toxic long-chain ammonium salts, PEO molecules are relatively inexpensive, nontoxic, and biodegradable.

Unlike ionic surfactants whose inorganic framework precursors cover the outer surface of the micelles, prior to polymerization, the synthesis of MSU-*X* implies first a dissolution of hydrophobic tetraethyl orthosilicate molecules (TEOS, $Si(OCH_2CH_3)_4$) into the outer hydrophilic volume built up by the long-chain poly(ethylene oxide) shell.

* To whom correspondence should be addressed. E-mail: prouzet@cit.enscm.fr.
† ENSCM.
‡ Delft University of Technology.
§ Michigan State University.

(1) Kresge, C. T.; Leonowicz, M. E.; Roth, W. J.; Vartuli, J. C.; Beck, J. S. *Nature* **1992**, *359*, 710.
(2) Beck, J. S.; Vartuli, J. C.; Roth, W. J.; Leonowicz, M. E.; Kresge, C. T.; Schmitt, K. D.; Chu, C. T.-W.; Olson, D. H.; Sheppard, E. W.; McCullen, S. B.; Higgins, J. B.; Schlenker, J. L. *J. Am. Chem. Soc.* **1992**, *114*, 10834.
(3) Inagaki, S.; Fukushima, Y.; Kuroda, K. *J. Chem. Soc., Chem. Commun.* **1993**, 680.
(4) Chen, C.-Y.; Li, H.-X.; Davis, M. E. *Microporous Mater.* **1993**, *2*, 17.
(5) Huo, Q.; Margolese, D. I.; Ciesla, U.; Demuth, D. G.; Feng, P.; Gier, T. E.; Sieger, P.; Firouzi, A.; Chmelka, B. F.; Schüth, F.; Stucky, G. D. *Chem. Mater.* **1994**, *6*, 1176.
(6) Huo, Q.; Margolese, D. I.; Ciesla, U.; Feng, P.; Gier, T. E.; Sieger, P.; Leon, R.; Petroff, P. M.; Schüth, F.; Stucky, G. D. *Nature* **1994**, *368*, 317.
(7) Antonelli, D. M.; Ying, J. Y. *Angew. Chem., Int. Ed. Eng.* **1996**, *35*, 426.
(8) Antonelli, D. M.; Ying, J. Y. *Chem. Mater.* **1996**, *8*, 874.
(9) Attard, G. S.; Glyde, J. C.; Göltner, C. G. *Nature* **1995**, *378*, 366.
(10) Attard, G. S.; Coleman, N. R. B.; Elliott, J. M. In *Mesoporous Molecular Sieves 1998*; Bonneviot, L., Beland, F., Danumah, C., Giasson, S., Kaliaguine, S., Eds.; Elsiever Science: Amsterdam, Lausanne, New York, Oxford, Shannon, Singapore, Tokyo, 1998; Vol. 117, p 89.
(11) Tanev, P., T.; Chibwe, M.; Pinnavaia, T. J. *Nature* **1994**, *368*, 321.
(12) Tanev, P., T.; Pinnavaia, T. J. *Science* **1995**, *267*, 865.
(13) Bagshaw, S. A.; Prouzet, E.; Pinnavaia, T. J. *Science* **1995**, *269*, 1242.
(14) Bagshaw, S. A.; Pinnavaia, T. J. *Angew. Chem., Int. Ed. Eng.* **1996**, *35*, 1102.
(15) Prouzet, E.; Pinnavaia, T. J. *Angew. Chem., Int. Ed. Eng.* **1997**, *36*, 516.
(16) Zhao, D.; Feng, J.; Huo, Q.; Melosh, N.; Fredrickson, G. H.; Chmelka, B. F.; Stucky, G. D. *Science* **1998**, *279*, 548.
(17) Zhao, D.; Huo, Q.; Feng, J.; Chmelka, B. F.; Stucky, G. D. *J. Am. Chem. Soc.* **1998**, *120*, 6024.
(18) Yang, P.; Deng, T.; Zhao, D.; Feng, P.; Pine, D.; Chmelka, B. F.; Whitesides, G. M.; Stucky, G. D. *Science* **1998**, *282*, 2244.

10.1021/cm9810281 CCC: $18.00
Published on Web 05/06/1999

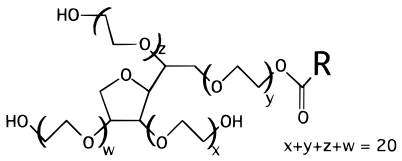

Tween 20 : Polyoxyethylene sorbitan monolaurate (R: $C_{11}H_{23}$)
Tween 40 : Polyoxyethylene sorbitan monopalmitate (R: $C_{15}H_{31}$)
Tween 60 : Polyoxyethylene sorbitan monostearate (R: $C_{17}H_{35}$)
Tween 80 : Polyoxyethylene sorbitan monooleate (R: $C_7H_{14}CH{=}CHC_8H_{17}$)

Figure 1. Structure of the ethoxylated sorbitan Tween surfactants. The EO groups are randomly distributed over the four available sites.

Until now, MSU-*X* silica molecular sieves have been prepared in neutral conditions using alkyl-PEO alcohols (MSU-1), alkyl−aryl-PEO surfactants (MSU-2), or poly(propylene oxide)−PEO block copolymers (MSU-3). We present herein a new group of mesoporous MSU silicas called MSU-4 silica, which were synthesized using the ethoxylated derivatives of the fatty esters of sorbitan, denoted Tween, an Atlas Co. trade name, as the structure-directing agents. Solvent-free sorbitan esters have been approved as food additives, and they are also used in shampoos, cosmetics, pharmaceuticals, and textiles.[19] Hence, they are widely used in biological systems, and they could help to expand the field of mesoporous materials to biological applications.

II. Experimental Section

MSU-4-type materials were synthesized in an open container from aqueous mixtures of TEOS, surfactant, and sodium fluoride as a mineralizer. The molar composition of each reaction mixture was Tween surfactant (noted Tw in the following), 0.02; TEOS, 0.16; NaF, 0.004, and H_2O, 55.6. In a typical preparation, 1.028 g of Tween 20 was first dissolved in 50 mL of water. Once surfactant dissolution was complete, 1.664 g of tetraethyl orthosilicate (TEOS) was added. The mixture was sonicated (power 20 W) at room temperature for 6 min. Once a milky homogeneous solution had been obtained, the mixture was left to stand overnight until a phase separation led to a colorless and transparent solution covered with a white foam that was removed before addition of NaF. It must be emphasized that, depending on the kind of sonication apparatus used, the sonication power required to allow this phase separation as the final product strucure may vary.[20] Sodium fluoride (0.84 mL of a 0.238 M NaF solution) was then added to the TEOS/surfactant solution to reach the molar ratio NaF/TEOS = 2%. The solution so obtained was aged under slow shaking at 35 °C for 48 h. A white colloidal suspension appeared progressively. The powder was filtered, dried, and calcined in air at 200 °C for 6 h and then at 620 °C for 6 h (5 °C·min^{-1}). The hydrophobic chain length effect was studied on three ethoxylated sorbitan esters, namely, the series of monolaurate (Tw-20), monopalmitate (Tw-40), and monostearate (Tw-60) (Figure 1). The monooleate (Tw-80), which only differs from Tw-60 by a double bond in the alkyl chain, was also tested. Tw-*X* (*X* = 20, 40, 60, 80) templated materials will be designated Tw-*X*−MSU-4 in the following.

All materials were characterized by scanning electron microscopy (SEM), small-angle X-ray scattering (SAXS), nitrogen adsorption at 77 K, and transmission electron microscopy (TEM). SAXS patterns were recorded on the D24 beamline of the DCI synchrotron ring located at LURE (France). The energy was monochromatized at 0.15 nm, and the detector was set at 143.7 cm from the sample prepared by mixing powders in paraffin oil. TEM was performed using a Philips CM30 T electron microscope with a LaB_6 filament as a source of electrons operated at 300 kV. Samples were mounted on a microgrid carbon polymer supported on a copper grid by placing a few droplets of a suspension of ground sample in ethanol on the grid, followed by drying at ambient conditions. SEM micrographs were obtained on a Hitachi S-5400 FEG microscope.

Nitrogen adsorption isotherms were measured at 77 K on a Micromeretics 2010 sorptometer using standard continuous procedures, and samples were first degassed at 150 °C for 15 h. Surface areas were determined by the BET method in the 0.05−0.2 relative pressure range,[21,22] and the pore size distribution was determined by the Broekhoff and de Boer (BdB) method.[23] It has been shown that accurate pore size determination can be obtained after correction of the Kelvin equation,[24,25] but the accuracy of the BdB correction for the pore size determination of mesoporous materials had been previously demonstrated by Galarneau et al.[25]

The correlation between pore size distribution (Å) and the nitrogen partial pressure has been calculated by Broekhoff and de Boer,[23] but we fitted this relationship by an eighth-degree polynomial to simplify further analysis. This polynomial value is given in the following expression:

$$y = 50.316 - 886.89x + 10393x^2 - 60448x^3 + (2.0507 \times 10^5)x^4 - (4.1856 \times 10^5)x^5 + (5.068 \times 10^5)x^6 - (3.3523 \times 10^5)x^7 + 93526x^8 \quad (R = 1) \quad (1)$$

with x = experimental nitrogen relative pressure and y = pore diameter (Å). The pore size distribution was then calculated by reporting the first derivative of the adsorbed volume of the desorption curve, which is at the thermodynamic equilibrium, as a function of the pore diameter calculated from eq 1.

The textural pore size was also evaluated from SEM observations and nitrogen adsorption isotherms. Indeed, we expect the interparticle porosity with a mean pore diameter d to be linked to the average diameter of particles D and the textural porosity ϵ on the basis of the following equation:[26]

$$d = \frac{2\epsilon D}{3(1-\epsilon)} \quad (2)$$

The particle size D was evaluated from SEM, but the textural porosity ϵ had to be determined from an estimation of the interparticle volume V_{tp}. For this purpose, we assumed that the adsorbed nitrogen volume above $P/P_o = 0.7$ was only arising from textural porosity. The interparticle volume V_{tp} (cm^3/g) was then calculated by dividing the gaseous adsorbed nitrogen volume at STP between $0.7 < P/P_o < 1.0$ by 646 (the ratio between gaseous and liquid volumes). The textural porosity ϵ was calculated on the basis of the MCM-41 mean density of 0.83 g·cm^{-3} (that is, a volume of 1.2 cm^3·g^{-1}) calculated by Edler et al.[27] This density includes the dense amorphous silica density (2.2 g·cm^{-3}) and the framework

(19) Porter, M. R. *Handbook of Surfactants*, 2nd ed.; Chapman & Hall: London, U.K., 1992; p 227.
(20) Cot, F.; Kooyman, P. J.; Larbot, A.; Prouzet, E. In *Mesoporous Molecular Sieves 1998*; Bonneviot, L., Beland, F., Danumah, C., Giasson, S., Kaliaguine, S., Eds.; Elsiever Science: Amsterdam, Lausanne, New York, Oxford, Shannon, Singapore, Tokyo, 1998; Vol. 117, p 231.
(21) Brunnauer, S.; Emmet, P. H.; Teller, E. *J. Am. Chem. Soc.* **1938**, *60*, 309.
(22) Brunnauer, S.; Deming, L. S.; Deming, W. S.; Teller, E. *J. Am. Chem. Soc.* **1940**, *62*, 1723.
(23) Broekhoff, J. C. P.; de Boer, J. H. *J. Catal.* **1968**, *10*, 377.
(24) Jaroniec, M.; Kruk, M.; Sayari, A. In *Mesoporous Molecular Sieves 1998*; Bonneviot, L., Beland, F., Danumah, C., Giasson, S., Kaliaguine, S., Eds.; Elsiever Science: Amsterdam, Lausanne, New York, Oxford, Shannon, Singapore, Tokyo, 1998; Vol. 117, p 325.
(25) Galarneau, A.; Desplantier, D.; Dutartre, R.; Di Renzo, F. *Mesoporous Mater.* **1999**, *27*, 297.
(26) Charpin, J.; Rasneur, B. *Tech. Ing.* **1987**, *1*, 1050.
(27) Edler, K. J.; Reynolds, P. A.; White, J. W.; Cookson, D. *J. Chem. Soc., Faraday Trans.* **1997**, *93*, 199.

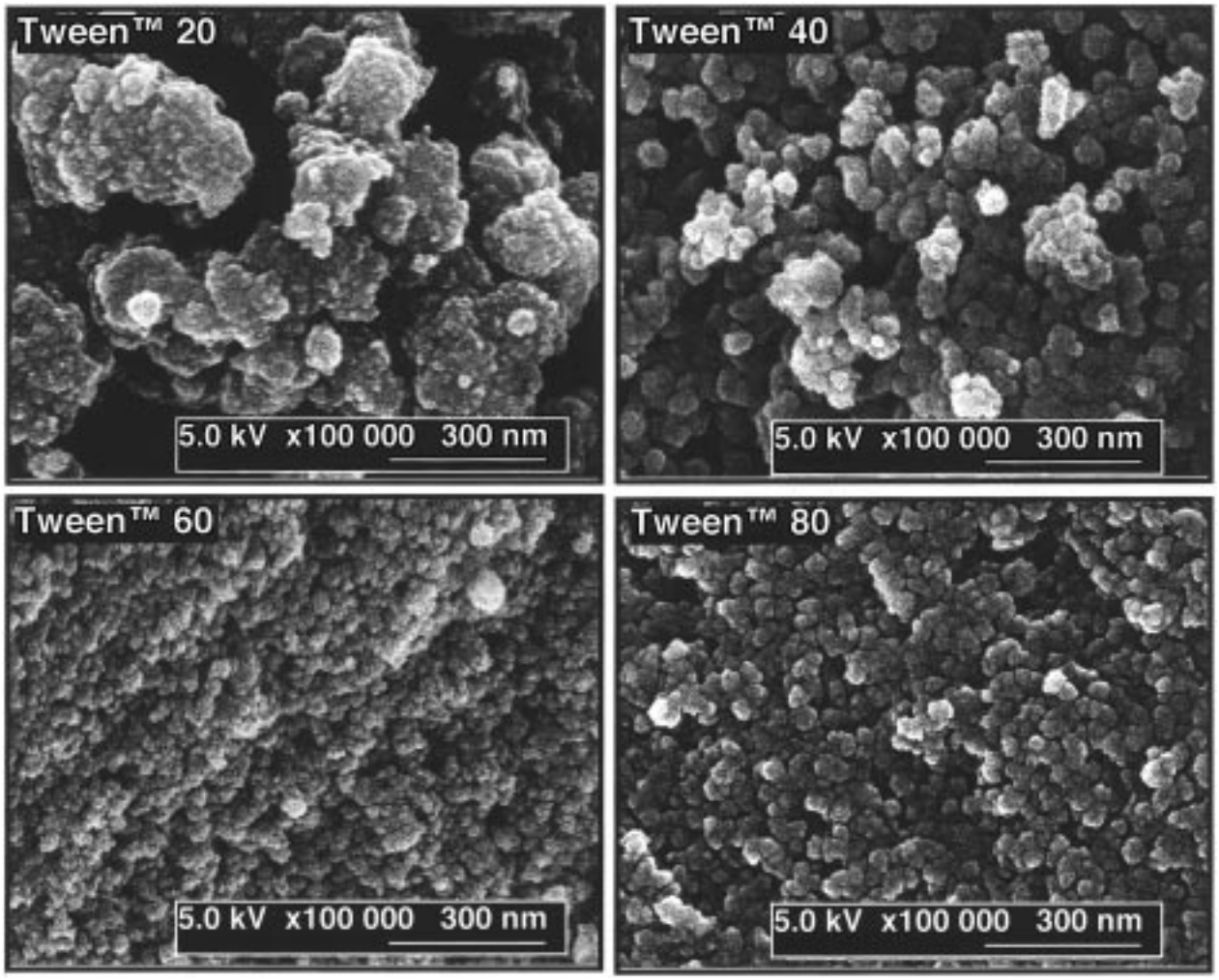

Figure 2. SEM observation of calcined powders synthesized with the four different ethoxylated sorbitan molecules.

porous volume. The textural porosity ϵ (%) was finally calculated according to the formula

$$\epsilon = 100V_{tp}/(1.2 + V_{tp}) \quad (3)$$

III. Results

SEM images showing the particle texture of MSU-4 silicas are displayed in Figure 2. The material synthesized with Tw-20 exhibits a structure with large aggregates of about 500 nm built of smaller and ill-defined elementary particles. Unlike Tw-20, the other surfactants, especially Tw-40 and Tw-80, provide MSU-4 silicas with well-defined elementary spherical particles with mean sizes of 60 nm (Tw-40), 30 nm (Tw-60), and 45 nm (Tw-80). These particles are much smaller than usually obtained with MCM-41-type materials (mean size $\sim$2 μm).[1] Consequently, they are expected to provide a significant textural porosity within almost the same size range.

SAXS patterns are displayed in Figure 3 , and *d* spacings are presented in Table 1. The patterns resemble those obtained with MSU-*X* materials with a single correlation peak due to the 3D wormhole porous framework structure.[13] A broad peak is also observed near 0.2 Å^{-1}. Analyses are in progress to identify this second diffraction feature, which cannot be assigned to a disordered hexagonal framework, but could be related to the wormhole geometry of the porous framework. The

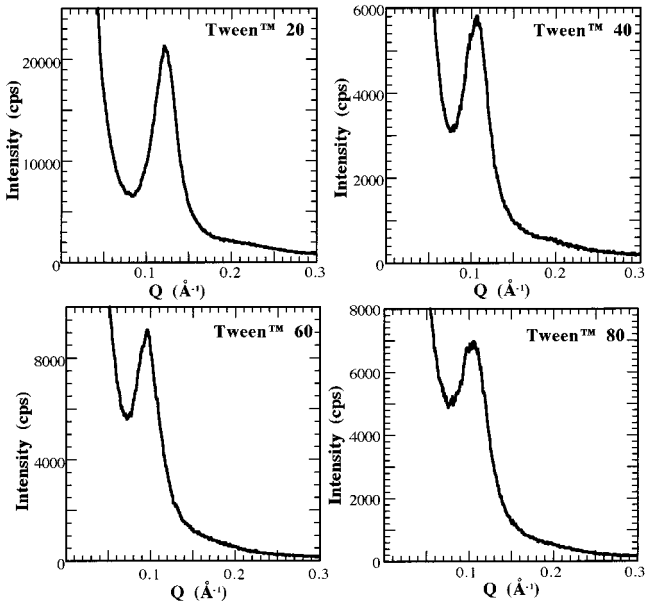

Figure 3. SAXS patterns of the calcined powders plotted versus the wave vector $Q = 2\pi/d$ (Å^{-1}).

lengths of the hydrophobic chain, from Tw-20 (R = $C_{11}H_{23}$) to Tw-60 (R = $C_{17}H_{35}$), are apparently marked by a parallel increase in the *d* spacing from 5.2 to 6.5 nm. Surprisingly, Tw-80 with an unsaturated $C_{17}H_{33}$ chain (see Figure 1), results in a pore size reduction

Table 1. Physicochemical Properties of Calcined MSU-4 Silica

template	*d* spacing (nm)	BET surface area ($m^2 \cdot g^{-1}$)	pore diam (framework/ textural) (nm)[a]	wall thickness (nm)[b]
Tw-20	5.2	773	3.4/>40	1.8
Tw-40	5.9	550	4.1/15−30	1.8
Tw-60	6.5	600	4.1/10−40	2.4
Tw-80	6.0	600	4.1/8−15	1.9

[a] BdB desorption average pore diameter. [b] Due to the disordered porous framework, the wall thickness had to be calculated by subtracting the pore diameter from the *d* spacing.[15]

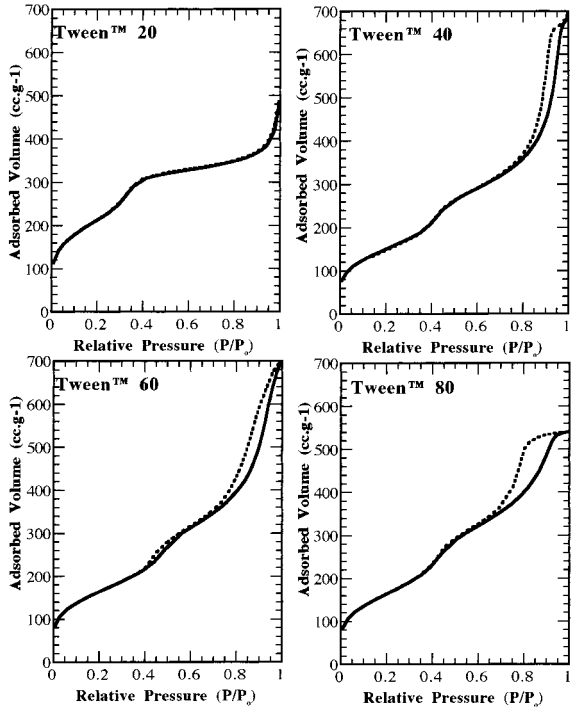

Figure 4. Nitrogen adsorption (continuous) and desorption (dashed) isotherms of the calcined powders.

relative to Tw-60. It appears that the normally observed correlation between the hydrophobic chain length and the *d* spacing[28] does not apply in our case.

The nitrogen adsorption isotherms are displayed in Figure 4. Characteristic of a mesoporous MTS-type material, the MSU-4 silicas all exhibit a step-shaped isotherm. In addition, the sorbitan surfactants clearly exhibit complementary interparticle (textural) and framework-confined (structural) porosity, as evidenced by the adsorption step and the uptake of N_2 above a partial pressure of 0.80. Surface areas determined by the BET method are close to 600 $m^2\ g^{-1}$ for all samples (see Table 1), and the BdB model applied to the desorption branch of the isotherms verifies the expected bimodal framework and textural pore size distributions (Figure 5). A closer comparison of the framework pore size distribution (see insets in Figure 5) shows that, except for the Tw-20−MSU-4 sample, which exhibits a smaller pore size (∼3.4 nm), the pore size distribution is the same for the other three compounds, with a mean size of 4.1 nm.

TEM observations on calcined materials (Figure 6) show different particle textures depending on the nature

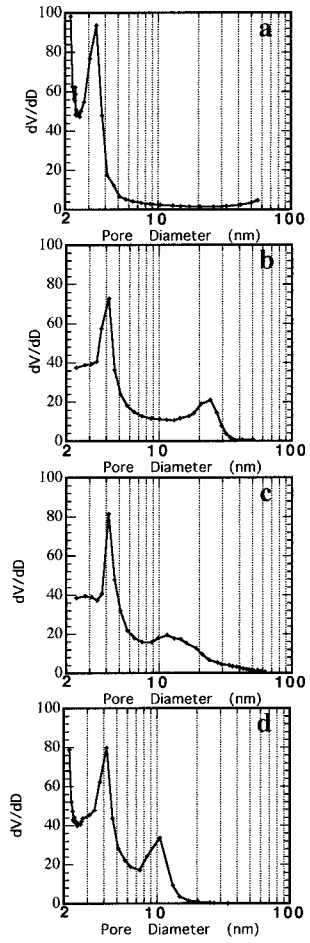

Figure 5. Pore size distribution deduced from the BdB model applied to the nitrogen desorption isotherm of the calcined powders: (a) Tw-20; (b) Tw-40; (c) Tw-60; (d) Tw-80. Inset: pore distribution in the 2−10 nm range.

of the surfactant. Tw-20−MSU-4 exhibits large aggregates of a framework with a 3D wormhole structure, analogous to previously reported MSU-1, -2, and -3 materials prepared from other PEO surfactants.[13,15] The textural pores are very large, in agreement with the N_2 adsorption isotherm that shows that Tw-20−MSU-4 exhibits a hysteresis loop at high partial pressure (Figure 4). In contrast to Tw-20−MSU-4, 20 nm well-defined textural pores are clearly seen in the TEM micrograph of Tw-40−MSU-4 (arrows in Figure 6, top right). This material contains ∼40 nm aggregated particles that are also observed by SEM (Figure 2). These particles, when packed upon drying, trap voids that provide the observed textural porosity. The TEM of Tw-60−MSU-4 (Figure 6, bottom left) exhibits large continuous areas of framework porous material. This is in contrast to SEM observations that show ∼30 nm particles and a nitrogen isotherm characteristic of a broad interparticle porosity between 10 and 40 nm. However, this pore size distribution is not as narrow as it is for the other compounds. Both the close packing of particles (see SEM photo) and the broadening of the textural pore size may explain why these voids are hardly distinguishable by TEM, which is a transmission technique. The biggest difference arises for Tw-80−MSU-4 (Figure 6, bottom right), where what appear to be aggregates of very small particles (<10 nm) of an ill-defined material are observed along with areas of

(28) Beck, J. S.; Vartuli, J. C.; Kennedy, G. J.; Kresge, C. T.; Roth, W. J.; Schramm, S. E. *Chem. Mater.* **1994**, *6*, 1816.

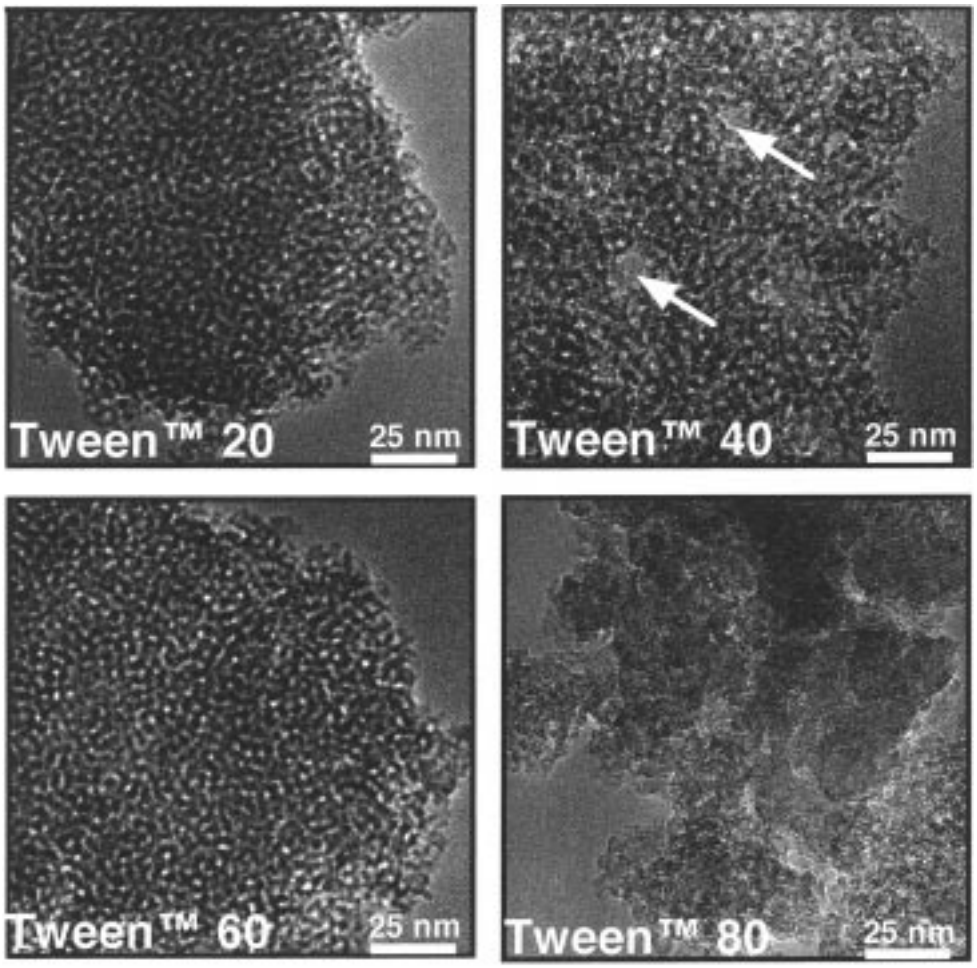

Figure 6. TEM observation of calcined powders synthesized with the four different ethoxylated sorbitan molecules (arrows point out interparticle spaces).

amorphous silica. The framework porosity is hardly distinguishable in this product.

IV. Discussion

IV.1. Origins of the Pore Size Variation. It is usually expected that changing the length of the hydrophobic chain on the surfactant allows one to modify the pore size of the final mesostructure.[2,28] This trend, which is typically observed for most mesostructure syntheses, seems not to hold rigorously for ethoxylated sorbitan structure directors. From Tw-20 to Tw-40, the 6 Å lengthening of the hydrophobic chain (C11−C15) should induce a pore diameter increase of 12 Å, whereas it is observed to be only 7 Å. Moreover, Tw-40−, Tw-60−, and Tw-80−MSU-4 exhibit the same framework pore size (4.1 nm). A comparison of *d* spacing, pore size, and wall thickness (Table 1) allows us to identify the origin of the *d* spacing variation with the surfactant chain length. From Tw-20 to Tw-40, the increase in *d* spacing is due to the pore size increase, as expected for an increase in the hydrophobic chain length, but the *d* spacing increase between Tw-40 and Tw-60 arises from a larger wall thickness (2.4 nm instead of 1.8 nm). From Tw-40 to Tw-60, the porous network remains unchanged (same pore size, surface area, and porous volume), but the silica framework becomes thicker. Finally, the same pore diameters and *d* spacings are found for Tw-80−MSU-4 as for Tw-40−MSU-4, even though the hydrophobic chain lengths are different. This led us to believe that the hydrophobic chain length has no effect on the final porosity. However, it appears from TEM images that Tw-80−MSU-4 is a material fundamentally different from the other members of the MSU-4 series. The 4 nm mesopores could be a consequence of the ordering of very small particles. In this case, the porosity could arise from interparticle spaces, and the diffraction peak observed in the X-ray pattern could be due to a correlation length related to the particle size, instead of a pore center to pore center distance. However, a spongelike structure consistent with the structure of the other members of the series cannot unequivocally be ruled out at this time.

IV.2. Textural Porosity. Large-particle mesostructures restrict access to framework mesopores in a way that could limit the catalytic process to the outermost regions of the particles. Tanev and Pinnavaia first pointed out that mesoporous materials with complementary textural macroporosity, such as those obtained through the amine-based neutral pathway, could be useful for improving catalytic processes.[12,29] From nitrogen adsorption isotherms, it appears that three of the MSU-4 mesostructures (Tw-40, -60, and -80) presented

(29) Pinnavaia, T. J.; Zhang, W. In *Mesoporous Molecular Sieves 1998*; Bonneviot, L., Beland, F., Danumah, C., Giasson, S., Kaliaguine, S., Eds.; Elsiever Science: Amsterdam, Lausanne, New York, Oxford, Shannon, Singapore, Tokyo, 1998; Vol. 117, p 23.

Table 2. Mean Interparticle (Textural) Porosity Mean Size Deduced from the Mean Particle Sizes and Textural Porosities

template	particle size (nm)[a]	total pore vol ($cm^3 \cdot g^{-1}$)	V_{tp}[b] ($cm^3 \cdot g^{-1}$)	ϵ (%)[c]	mean interparticle pore size (nm)[d]
Tw-20	n.o.[e]	0.75	0.23	16	>80[f]
Tw-40	60	1.06	0.57	32	19
Tw-60	30	1.08	0.53	31	9
Tw-80	45	0.84	0.26	18	7

[a] Direct SEM observation. [b] Deduced from the nitrogen adsorbed volume above $P/P_o = 0.7$. [c] $\epsilon = 100V_{tp}/(1.2 + V_{tp})$. [d] Calculated with eq 2. [e] n.o. = not observable. [f] Interaggregate pores deduced from SEM.

in this paper exhibit an appreciable textural porosity between 10 and >40 nm, even though the actual structure of Tw-80−MSU-4 remains questionable. The direct evaluation of the interparticle porosity from SEM observations (Table 2) fit rather well with the pore size distribution found by the BdB model (Table 1). For Tw-40, the TEM also allows a direct observation of such pores (Figure 6, top right). This comparison allows us to expect that MSU-4 silicas, particularly those obtained with Tw-40, -60, and -80, have small elementary particle sizes that provide significant interparticle porosity capable of facilitating framework access for catalytic applications.

IV.3. Reaction Mechanism. The nonionic (N^oI^o) PEO-based pathway to MTS materials is specific, because the surfactant not only contributes to the assembly mechanism but also acts as a hydrolysis catalyst for the TEOS molecules.[13,15] Unlike the approaches of Attard[9] and Stucky[16] who showed that mesostructure assembly with nonionic surfactants can occur through an electrostatic assembly mechanism when strong acidic conditions allow the PEO chains to be protonated, the assembly of MSU-*X* mesoporous materials occurs in a near-neutral pH range that usually corresponds to the lowest reactivity domain for TEOS hydrolysis.[30] MSU-1, -2, and -3 synthesized with alkyl, alkyl−aryl, and block copolymer surfactants, respectively, can be synthesized under these conditions, by simply mixing TEOS with the surfactant solution at room temperature. However, we also showed that fluoride ion is a powerful mineralizer that boosts the reaction rate and improves the structural quality of the final material without changing the pH of the solution.[13,15] For the present study, we also carried out syntheses with the different Tween surfactants without adding sodium fluoride. The products were less structured than those obtained with fluoride-assisted syntheses, and their X-ray pattern exhibited *d* spacings smaller than about 4.0 nm. It appeared also that the kinetics was slowed, with the reaction induction time shifted from 2 h after mixing up to more than 2 days. Moreover, absolutely no reaction occurred with Tw-80, which provides another example of the unsusual behavior of this surfactant. The addition of fluorine is thus a prerequisite to achieve an efficient catalysis of the first hydrolysis step, when Tween surfactants are used as templates. Unlike ethoxylated sorbitan monolaurate (Tween 20), tests with nonethoxylated sorbitan monolaurate (Span 20) and fluorine as a mineralizer did not give any ordered structure under equivalent reaction conditions. PEO groups appear thus to be required for the assembly process between TEOS hydrolysis products and surfactant.

Tween surfactants have a very special shape with a short hydrophobic chain compared with a large hydrophilic head made of three free PEO chains and one linking the ring to the hydrophobic tail. If we calculate the geometrical packing parameter $g = v/a_o l_c$[31,32] by assuming a full extension of these chains perpendicular to the hydrophobic tail, one finds $g \approx 0.08$ (v = chain volume = 92 Å^3, l_c = alkyl chain length = 13 Å, calculated with the alkyl chain diameter ~3 Å and the hydrophilic head diameter ~34 Å). This value is far below the spherical micelle geometrical parameter upper limit (1/3). When aggregated into micelles, these molecules most likely have their free PEO chains oriented as parallel as possible to the alkyl tail, so that a short (there are only five EO groups on average per chain) but dense hydrophilic shell around the hydrophobic core will arise. As this core may not be as close packed as with linear surfactant molecules, the inner volume may not depend directly on the hydrophobic tail length. The binding of silica to the hydrophilic shell[15] may alter the geometrical parameters, thus causing the pore size not to scale directly with the surfactant chain length.

V. Conclusion

In the expanding field of the micelle-templated structures, the extension of the syntheses using nonionic surfactants to a new MSU-*X* derivative, named MSU-4, based on ethoxylated sorbitan molecules provides materials with a significant textural porosity, which could help to overcome the previous limitations of large-particle mesostructures obtained from PEO surfactant assembly. Previously, only mesostructured HMS silicas prepared from neutral amine surfactants were known to exhibit complementary textural mesoporosity.[12] Indeed, shortening the average radius of particles from 1 μm, a typical size obtained with M41S materials, to ~20 nm increases the external particle surface area by 2500 and shortens the longest diffusion length by 50. All diffusion-limited processes should thus be boosted. These surfactants, which are biologically compatible, may also be useful for the synthesis of mesostructures suitable for the trapping of living cells. Finally, the sorbitan structure directors reported here have allowed us to approach a borderline area of mesostructure synthesis and point to the possibility of a new mechanism for MTS synthesis based on particle assembly as suggested for Tw-80−MSU-4. Particle assembly has also been recognized recently as a possible mechanism for the assembly of mesostructured tin oxide,[33] suggesting that this could become a general assembly pathway.

Acknowledgment. T.J.P. and E.P. acknowledge the partial support of this research through NSF-CRG Grant 96-33798 and NATO funding, and the LURE staff for help with the SAXS experiments.

CM9810281

(30) Brinker, C. J. *J. Non-Cryst. Solids* **1988**, *100*, 31.

(31) Israelachvili, J. N.; Mitchell, D. J.; Ninham, B. W. *J. Chem. Soc., Faraday Trans.* **1976**, *72*, 1525.

(32) Israelachvili, J. N.; Mitchell, D. J.; Ninham, B. W. *Biochim. Biophys. Acta* **1977**, *1977*, 185.

(33) Severin, K. G.; Abdel-Fattah, T. M.; Pinnavaia, T. J. *J. Chem. Soc., Chem. Commun.* **1998**, 1471.